

## RESEARCH ARTICLE

# Polycystin-1 regulates cardiomyocyte mitophagy

Andrea Ramírez-Sagredo<sup>1</sup>  | Clara Quiroga<sup>2</sup>  | Valeria Garrido-Moreno<sup>1</sup>  |  
 Camila López-Crisosto<sup>1,2</sup>  | Sebastian Leiva-Navarrete<sup>1,3,4</sup> |  
 Ignacio Norambuena-Soto<sup>1</sup>  | Jafet Ortiz-Quintero<sup>1,5</sup> | Magda C. Díaz-Vesga<sup>1,6,7</sup>  |  
 William Perez<sup>8</sup>  | Troy Hendrickson<sup>8,9</sup>  | Valentina Parra<sup>1,3,4</sup>  |  
 Zully Pedrozo<sup>1,4,6</sup>  | Francisco Altamirano<sup>8,10</sup>  | Mario Chiong<sup>1</sup>  |  
 Sergio Lavandero<sup>1,11,12</sup> 

<sup>1</sup>Advanced Center of Chronic Diseases (ACCDiS), Facultad de Ciencias Químicas y Farmacéuticas y Facultad de Medicina, Universidad de Chile, Santiago, Chile

<sup>2</sup>Advanced Center for Chronic Diseases (ACCDiS), División de Enfermedades Cardiovasculares, Facultad de Medicina, Pontificia Universidad Católica de Chile, Santiago, Chile

<sup>3</sup>Autophagy Research Center, Universidad de Chile, Santiago, Chile

<sup>4</sup>Network for the Study of High-lethality Cardiopulmonary Diseases (REECPAL), Universidad de Chile, Santiago, Chile

<sup>5</sup>Departamento de Bioanálisis e Inmunología, Escuela de Microbiología, Facultad de Ciencias, Universidad Nacional Autónoma de Honduras, Tegucigalpa, Honduras

<sup>6</sup>Programa de Fisiología y Biofísica, ICBM, Facultad de Medicina, Universidad de Chile, Santiago, Chile

<sup>7</sup>Grupo de Investigación en Ciencias Básicas y Clínicas de la Salud, Pontificia Universidad Javeriana de Cali, Cali, Colombia

<sup>8</sup>Department of Cardiovascular Sciences, Houston Methodist Research Institute, Houston, TX, USA

<sup>9</sup>Texas A&M MD/PhD Program, Texas A&M Health Science Center, College Station, TX, USA

<sup>10</sup>Department of Cardiothoracic Surgery, Weill Cornell Medical College, Cornell University, Ithaca, NY, USA

<sup>11</sup>Corporación Centro de Estudios Científicos de las Enfermedades Crónicas (CECEC), Santiago, Chile

<sup>12</sup>Department of Internal Medicine, Cardiology Division, University of Texas Southwestern Medical Center, Dallas, TX, USA

## Correspondence

Sergio Lavandero, Advanced Center of Chronic Diseases (ACCDiS), Facultad de Ciencias Químicas y Farmacéuticas & Facultad de Medicina, Universidad

## Abstract

Polycystin-1 (PC1) is a transmembrane protein found in different cell types, including cardiomyocytes. Alterations in PC1 expression have been linked to mitochondrial damage in renal tubule cells and in patients with autosomal dominant polycystic kidney disease. However, to date, the regulatory role of PC1 in cardiomyocyte mitochondria is not well understood. The analysis of mitochondrial morphology from cardiomyocytes of heterozygous PC1 mice (PDK1<sup>+/-</sup>) using transmission electron microscopy showed that cardiomyocyte mitochondria were smaller with

**Abbreviations:** ADPKD, autosomal dominant polycystic kidney disease; ATP5A, ATP synthase F1 subunit alpha; CQ, chloroquine; MTCO1, mitochondrially encoded cytochrome c oxidase I; NDUF8, NADH dehydrogenase [ubiquinone] 1 beta subcomplex subunit 8; NRVM, neonatal rat ventricular myocytes; OXPHOS, oxidative phosphorylation; PC1, polycystin-1; SDHB, succinate dehydrogenase complex iron sulfur subunit B; UQCRC2, cytochrome b-c1 complex subunit 2.

Andrea Ramirez-Sagredo and Clara Quiroga contributed equally to this study.

This is an open access article under the terms of the Creative Commons Attribution-NonCommercial-NoDerivs License, which permits use and distribution in any medium, provided the original work is properly cited, the use is non-commercial and no modifications or adaptations are made.

© 2021 The Authors. *The FASEB Journal* published by Wiley Periodicals LLC on behalf of Federation of American Societies for Experimental Biology

de Chile, Olivos 1007, 8380492,  
Santiago, Chile.  
Email: slavander@uchile.cl

### Funding information

Agencia Nacional de Investigación y Desarrollo (ANID), Chile, Grant/Award Number: FONDECYT 3190546, 1190743, 1200490, FONDAPE 15130011 and 21171588; International Centre for Genetic Engineering and Biotechnology (ICGEB), Grant/Award Number: CRP/CHL18-04; University of Chile grant U-Redes Generación, Grant/Award Number: VID G\_2018-35

increased mitochondria density and circularity. These parameters were consistent with mitochondrial fission. We knocked-down PC1 in cultured rat cardiomyocytes and human-induced pluripotent stem cells (iPSC)-derived cardiomyocytes to evaluate mitochondrial function and morphology. The results showed that down-regulation of PC1 expression results in reduced protein levels of sub-units of the OXPHOS complexes and less functional mitochondria (reduction of mitochondrial membrane potential, mitochondrial respiration, and ATP production). This mitochondrial dysfunction activates the elimination of defective mitochondria by mitophagy, assessed by an increase of autophagosome adapter protein LC3B and the recruitment of the Parkin protein to the mitochondria. siRNA-mediated PC1 knockdown leads to a loss of the connectivity of the mitochondrial network and a greater number of mitochondria per cell, but of smaller sizes, which characterizes mitochondrial fission. PC1 silencing also deregulates the AKT-FoxO1 signaling pathway, which is involved in the regulation of mitochondrial metabolism, mitochondrial morphology, and processes that are part of cell quality control, such as mitophagy. Together, these data provide new insights about the controls that PC1 exerts on mitochondrial morphology and function in cultured cardiomyocytes dependent on the AKT-FoxO1 signaling pathway.

### KEYWORDS

cardiomyocyte, FoxO1, mitochondrial dynamics, mitochondrial metabolism, mitophagy, polycystin-1

## 1 | INTRODUCTION

Autosomal dominant polycystic kidney disease (ADPKD) is the most common genetic cause of end-stage renal disease, affecting 1 in 1000 people worldwide.<sup>1</sup> It is generated as a result of mutations in the *PKD1* and *PKD2* genes encoding polycystin-1 (PC1) and -2 (PC2),<sup>2</sup> altering their function and leading to the formation of renal cysts, deterioration of renal function, and ultimately, renal insufficiency.<sup>3</sup> A series of extrarenal symptoms are detected before the occurrence of renal cysts,<sup>4,5</sup> which even have led to finding that the main responsible factors for morbidity and mortality of ADPKD patients are cardiovascular events.<sup>6</sup>

Studies have shown that cardiomyocyte-specific PC1 knockout mice exhibited decreased cardiac contractility and low levels of L-type calcium channel protein,<sup>7</sup> and that PC1 ablation reduces the duration of the action potential in cardiomyocytes.<sup>3</sup>

Recent evidence has suggested that PC1 downregulation participates in cellular metabolic dysregulation in kidney tissue of an ADPKD murine model,<sup>8-10</sup> with structural and functional mitochondrial alterations.<sup>3,8,10-12</sup> However, until now, it is unclear if these mitochondrial disorders occur in the heart.

The transcriptional factors Forkhead box protein O (FoxO) are crucial regulators of energetic metabolism through their function in the liver, skeletal and cardiac muscle, adipose tissue, and pancreas.<sup>13-15</sup> These factors regulate many genes and modulate several cellular functions, including cell cycle, apoptosis, DNA damage repair, and metabolism.<sup>16,17</sup> FoxO1, like other members of this family, is expressed ubiquitously in mammals<sup>16-18</sup> and finely regulated through a series of posttranslational modifications, being negatively regulated in the presence of insulin or growth factors that activate protein kinase AKT. This AKT-dependent FoxO phosphorylation triggers its cytoplasmic relocalization, inactivation, and proteasomal degradation.<sup>19</sup> Interestingly, regulation of heart contractility by PC1 on L-type calcium channels has been linked to the AKT signaling pathway.<sup>7,20</sup>

Mitochondria play an essential role in both the life and death of cardiomyocytes. In healthy cells, they supply necessary ATP, through oxidative phosphorylation, to respond to the high energy demand of the heart. Moreover, mitochondria are also relevant regulators of cell death, responding to a wide variety of stress signals. Changes in mitochondria number, shape, structure, and function have been associated with the development of cardiovascular diseases.<sup>12,21</sup> The shape and function of the mitochondrial network are finely

regulated by two dynamic and opposing processes known as mitochondrial fusion and fission.<sup>21,22</sup> In addition, the mitochondria have a quality control mechanism for the correct functioning of both processes, where, in the event of a sustained imbalance in any of them, the process of selective elimination of defective mitochondria known as mitophagy is activated.<sup>23,24</sup> Dysregulation of the balance between fusion and fission processes and mitophagy may lead cells to mitochondrial metabolism alterations by the over-representation of fragmented organelles.<sup>12,22,25,26</sup> In this context, some studies have shown that mitochondrial dynamics and function are also regulated by FoxO1.<sup>16-18</sup>

The present study was aimed to investigate whether alterations of PC1 expression trigger changes in the AKT/FoxO1 signaling pathway, mitochondrial dynamics and function, and the activation of the mitophagy machinery in primary cultured rat cardiomyocytes and human iPSC-derived cardiomyocytes.

## 2 | MATERIALS AND METHODS

### 2.1 | Reagents

Anti-Polycystin-1 and anti-GAPDH antibodies were obtained from Santa Cruz (Dallas, TX, USA), whereas anti-mtHsp70, anti-PINK1, anti-Parkin, anti-LC3B, and anti-total OXPHOS antibodies were obtained from Abcam (Cambridge, UK). Anti-phospho-Drp1, anti-Drp-1, anti-MFN2, anti-OPA1, anti-phospho-AKT, anti-AKT, anti-phospho-FoxO1, and anti-FoxO1 antibodies were obtained from Cell Signaling Technology (Danvers, MA, USA). Anti-mtHsp70 antibody, Tetramethylrhodamine methyl ester (TMRM), mitotracker-green FM, CellROX Orange Reagent, fetal bovine serum (FBS), newborn calf serum (NBCS), Alexa secondary antibodies, RNAiMax, Opti-MEM, Trizol, T-Ripa, PowerUp SYBR Green Master Mix, and DNazol reagents were obtained from Thermo Fisher Scientific (Waltham, MA, USA). The antibody against  $\beta$ -tubulin, oligomycin, dihydrorhodamine-123, carbonyl cyanide *m*-chlorophenylhydrazone (CCCP), Dulbecco's modified Eagle's medium (DMEM), M199, 5-bromo-2'-deoxyuridine (BrdU), and Mission siRNA against PC1 were obtained from Sigma-Aldrich (St. Louis, MI, USA). Phosphatase and protease inhibitor cocktails were obtained from Roche (Basel, Switzerland). The Cell Titer-Glo Kit was obtained from Promega Corporation (Madison, WI, USA). Protein assay and iScript reagents were obtained from Bio-Rad (Hercules, CA, USA). Adenovirus FoxO1-GFP and FoxO1-CA-GFP were kindly provided by Dr Joseph A. Hill (University of Texas Southwestern Medical Center, Dallas). Organic and inorganic compounds, acids, and solvents were obtained from Merck (Darmstadt, Germany).

### 2.2 | Animals

All animal care and experimental procedures complied with Public Health Service Policy on Humane Care and Use of Laboratory Animals and the ILAR Guide for Care and Use of Laboratory Animals, published by the National Research Council of The National Academies, and were approved by the Institutional Ethics Review Committees from Universidad de Chile (Ethics Number: CBE2013-04). Heterozygous PDK<sup>+/-</sup> mice were obtained by crossing cardio-specific PC-1 knockout (PDK<sup>-/-</sup>) mice<sup>7</sup> with wild-type (PDK<sup>+/+</sup>) mice.

### 2.3 | Cardiomyocyte culture and transfections

Neonatal rat ventricular myocytes (NRVMs) were isolated from hearts of 1- to 2-day-old Sprague Dawley rats, as described previously.<sup>27</sup> Cells were plated and cultured for 24 hours in DMEM:M199 (4:1) containing 5% FBS, 10% NBCS, 100  $\mu$ M BrdU, and antibiotics. For PC1 and FoxO1 knockdown, NRVMs were transfected overnight with siRNAs specific for PC1 or FoxO1 (120 nM) with lipofectamine RNAiMax in Opti-MEM. Scrambled siRNA (siScr) was used as a control of transduction. After 24 hours, cells were harvested in TRIzol or T-Ripa containing phosphatase and protease inhibitors for harvesting mRNA or protein, respectively. To induce overexpression of constitutively active FoxO1 (FoxO1-CA)-green fluorescent protein (GFP), cardiomyocytes were transduced with adenoviral vectors (Ad-FoxO1-CA-GFP) at a multiplicity of transduction (MOI) of 10 and 25, at least for 24 hours. Adenovirus GFP (Ad-GFP) was used as a control of transduction.

Cardiomyocytes were differentiated using a commercially available human iPSC line (Thermo Scientific, A18945) as described.<sup>3</sup> Human iPSC-derived cardiomyocytes were cultured for 80+ days to increase the ventricular population (MLC2v-positive cells). For imaging experiments, cardiomyocytes were plated on imaging culture slides (ten compartment Cellview, Greiner Bio-One) coated with Matrigel (1:100) and maintained for 4 days with RPMI+B27 (Thermo Fisher). On the fifth day, cardiomyocytes were infected with CellLight Mitochondria-GFP, BacMam 2.0 (Thermo Fisher, #C10508) for 1 hour at room temperature and 23 hours at 37°C. After 24 hours, culture media was replaced with new RPMI+B27 (Thermo Fisher) and cells were transfected using control and PC1 siRNA (Mission Sigma) with lipofectamine RNAiMAX (Thermo Fisher). A confocal microscope Olympus FV-3000 was used to obtain mitochondria z-stacks.

## 2.4 | Western blot analysis

Cells were washed with PBS and lysed using T-Ripa lysis buffer (10 mM Tris-HCl pH 7.4; 5 mM EDTA; 50 mM NaCl; 1% v/v Triton X-100; aprotinin 20 mg/mL; leupeptin 1 mg/mL; phenylmethylsulfonyl fluoride 1 mM; and  $\text{Na}_3\text{VO}_4$  1 mM). Protein concentration was determined using the Bradford method and then, equal amounts of protein from cells were separated by SDS-PAGE (10% polyacrylamide gels), electrotransferred to nitrocellulose membranes, and blocked with 5% fat-free milk in Tris-buffered saline (pH 7.6) containing 0.1% (v/v) Tween-20 (TBST). Membranes were sequentially incubated with the following primary antibodies: anti-PC1 (1:500), anti-PINK1 (1:1000), anti-Parkin (1:1000), anti-LC3B (1:1000), anti-total OXPHOS (1:500), anti-phospho-Drp1 (1:1000), anti-Drp-1 (1:1000), anti-MFN2 (1:1000), anti-OPA1 (1:1000), anti-phospho-AKT (1:1000), anti-AKT (1:1000), anti-phospho-FoxO1 (1:1000), anti-FoxO1 (1:1000), anti- $\beta$ -tubulin (1:2000), anti-GAPDH (1:5000), and horseradish peroxidase-linked secondary antibodies [1:5000 in 1% (w/v) milk in TBST]. Luminescence was detected using ECL solution, visualized and digitalized using a Syngene Scanner (Syngene, Cambridge, UK), and quantified with the ImageJ software. Protein content was normalized to  $\beta$ -tubulin or GAPDH levels.

## 2.5 | Total RNA extraction and reverse transcription

Total RNA was extracted from cultured cardiomyocytes using the TRIzol reagent. RNA samples were quantified and their absorbance 260/280 was measured by NanoDrop (Thermo Fisher Scientific, Waltham, MA, USA). Reverse transcription was performed using 1  $\mu\text{g}$  of RNA and 1  $\mu\text{g}$  of total RNA and iScript Reverse Transcription Supermix, using the RT-qPCR kit (BIO-RAD).

## 2.6 | Mitochondrial DNA extraction

Total DNA was isolated from cultured cardiomyocytes using the DNazol reagent (Thermo Fisher Scientific). Mitochondrial DNA copy number was estimated by qPCR by comparing the abundance of the mitochondrial *cytochrome b* gene to that of the nuclear  $\beta$ -actin gene, as described previously.<sup>28</sup>

## 2.7 | Real-time PCR

RT-qPCR was performed using specific primers designed for rats (Table S1) and PowerUp SYBR Green Master Mix (Life

Technologies) in a StepOnePlus Real-Time PCR System. The  $2^{-\Delta\Delta\text{Ct}}$  method was used to analyze the data. The values for each target gene were normalized to 18S rRNA gene expression levels.

## 2.8 | Mitochondrial membrane potential ( $\Psi_m$ )

$\Psi_m$  was measured after loading cardiomyocytes with 200 nM tetramethylrhodamine methyl ester during 30 minutes (excitation: 543 nm, emission: over 560 nm), as previously described.<sup>29</sup> Cell fluorescence was determined by flow cytometry using an FACScan system (Becton Dickinson, San Jose, CA, USA). Carbonyl cyanide *m*-chlorophenylhydrazone (CCCP; 50  $\mu\text{M}$ ) decoupling agent was used as a control 30 minutes prior to measurement.

## 2.9 | ATP measurement

Cells were plated in gelatin-coated 96-well plates and ATP content was determined using a luciferin/luciferase-based assay.<sup>30</sup> For the measurement of relative intracellular ATP levels, the medium was removed and replaced by Krebs medium with  $\text{Ca}^{2+}$  to then use the Cell Titer-Glo Kit, according to the manufacturer's instructions. As a control, 200 nM oligomycin was used. Subsequently, the cell lysates were transferred to a 96-well plate and analyzed on an In Vivo FX Pro (Bruker, Billerica, MA, USA).

## 2.10 | Oxygen consumption determination in live cells

Cardiomyocytes plated on 60-mm gelatin-coated dishes were trypsinized and then re-suspended in PBS. Cells were placed in a sealed chamber at 25°C, coupled to a Clark electrode (Yellow Springs Instruments, Fisher Scientific, Pittsburgh, PA, USA). To determine the maximum oxygen consumption rate, 50  $\mu\text{M}$  CCCP was added to the NRVM.<sup>21</sup> The electrode detects the amount of oxygen remaining in the chamber in time. Cells were maintained in the chamber for 20 minutes to calculate the rate of oxygen consumption. The values were averaged and expressed relative to the oxygen consumption of controls.

## 2.11 | Immunofluorescence and Parkin/mtHsp70 colocalization

Cells were cultured on gelatin-coated coverslips and fixed with PBS containing 4% paraformaldehyde, incubated for



10 minutes in ice-cold 0.1%, permeabilized with Triton X-100 for 15 minutes, and blocked with 1% BSA in PBS for 1 hour. The cells were then incubated overnight with antibodies against Parkin (1:500) and mtHsp-70 (1:500) and then with the secondary antibodies Alexa Fluor 456-conjugated anti-rabbit-IgG (1:600) and Alexa Fluor 488-conjugated anti-mouse-IgG for Parkin and mtHsp70, respectively. For colocalization, only one focal plane was analyzed with a Pascal 5 Axiovert 200 laser scanning microscope (Zeiss, Oberkochen, Germany). Images obtained were deconvolved, and background was subtracted using the ImageJ software. Colocalization between the proteins was quantified using the Manders' algorithm.<sup>21,31</sup>

## 2.12 | Mitochondrial dynamics

NRVM and human iPSC-derived cardiomyocytes were incubated for 30 minutes with 400 nM of Mitotracker Green FM and Krebs medium with  $\text{Ca}^{2+}$ . Confocal image stacks were obtained with a Pascal 5 Axiovert 200 laser scanning microscope (Zeiss, Oberkochen, Germany) using Plan-Apochromat 63 × 1.4 NA oil DIC objective and captured using LSM5 v3.2 image and analysis software.<sup>21</sup> Images were deconvolved with the ImageJ software, and then z-stacks of thresholded images were used for 3D reconstitution using the ImageJ-VolumeJ plug-in.<sup>21</sup> The number of mitochondria and individual volume of each mitochondrion were quantified using the ImageJ-3D Object counter plug-in.<sup>21</sup> The values of individual mitochondrial volumes were averaged and expressed relative to controls. The decrease of mitochondrial volume mean, in conjunction with an increase in the number of mitochondria, was considered as fission criteria.<sup>21,31</sup> Each experiment was performed at least five times, and 20 cells were quantified per condition.

## 2.13 | Transmission electron microscopy specimen processing and imaging

Heterozygous  $\text{Pkd1}^{+/-}$  ( $n = 3$ ) and  $\text{Pkd1}^{+/+}$  (controls,  $n = 3$ ) mice (9 to 12 weeks old) were anesthetized with isoflurane (Baxter Healthcare) and subsequently, cervical dislocation was performed. Then, a thoracotomy was conducted, and hearts were rapidly extracted. Whole mice hearts underwent retrograde perfusion with fixative solution (2% paraformaldehyde and 2.5% glutaraldehyde in 0.1 M sodium cacodylate buffer and 50 mM  $\text{CaCl}_2$ , pH 7.4) at 3 mL per min at room temperature for 15 minutes before being stored at 4°C in fixative solution. Sections from left ventricle were obtained from hearts and were post-fixed using  $\text{OsO}_4$  (2%  $\text{OsO}_4$  + 0.8%

$\text{K}_3\text{Fe}(\text{CN})_6$  in 0.1 M cacodylate buffer pH 7.4). Then, each segment underwent sequential dehydration using different concentrations of ethanol and embedded in Epoxy resin.<sup>32</sup> Ultrathin sections were cut using a Leica Ultracut R microtome. Images were acquired at 11500X, 13500X, and 26500X magnification using a transmission electron microscope Philips Tecnai 12 (Biotwin) equipped with capture software iTEM Olympus Soft Imaging solutions (Windows NT 6.1). In total, 858 mitochondria were evaluated, with a minimum of 5 and a maximum of 27 mitochondria per image. Cells with intact fibers were selected for the analysis. Each mitochondrion was traced using the Multi measure ROI tool of ImageJ (National Institutes of Health, V. 1.5) as described.<sup>33,34</sup> Shape descriptors of individual mitochondria were measured in 2D including: (a) surface area (expressed as  $\mu\text{m}^2$ ); (b) perimeter (the distance surrounding the actual shape of mitochondria in 2D, expressed in  $\mu\text{m}$ ); (c) circularity (calculated by the formula:  $4\pi \times \text{area}/\text{perimeter}^2$ ). Mitochondria exhibiting a perfect circular shape have a circularity value close to 1.0, whereas more elongated mitochondria have a circularity value that is closer to 0.0; and (d) density (calculated by the formula: numbers of mitochondria/area).

## 2.14 | Statistical analysis

The results are presented as mean  $\pm$  SEM, using the Student's *t* test for direct comparisons and one-way or two-way analysis of variance with Tukey's post-test for multiple comparisons. A value of  $P < .05$  was considered to be statistically significant. Statistical analysis of all experiments was performed using GraphPad Prism 6 (GraphPad 182 Software, Inc, La Jolla, CA, USA).

# 3 | RESULTS

## 3.1 | PC1 silencing induces loss of mitochondrial functionality

Given that the PDK1 mutation induces alterations of metabolism in kidney cell lines,<sup>1,11,35</sup> we evaluated the functional state of mitochondria and oxidative metabolism markers in PC1 knocked-down cardiac cells, specifically in NRVM. In these cells, we used a specific siRNA against PC1 (siPC1) and determined a reduction of 50% in both mRNA and protein levels of PC1 (Figure S1A). We also obtained human iPSC-derived cardiomyocytes (Figure S1B). In these cells, siPC1 also reduced the protein levels of PC1 by around 50% (Figure S1C). This reduction was sufficient to decrease the mitochondrial membrane

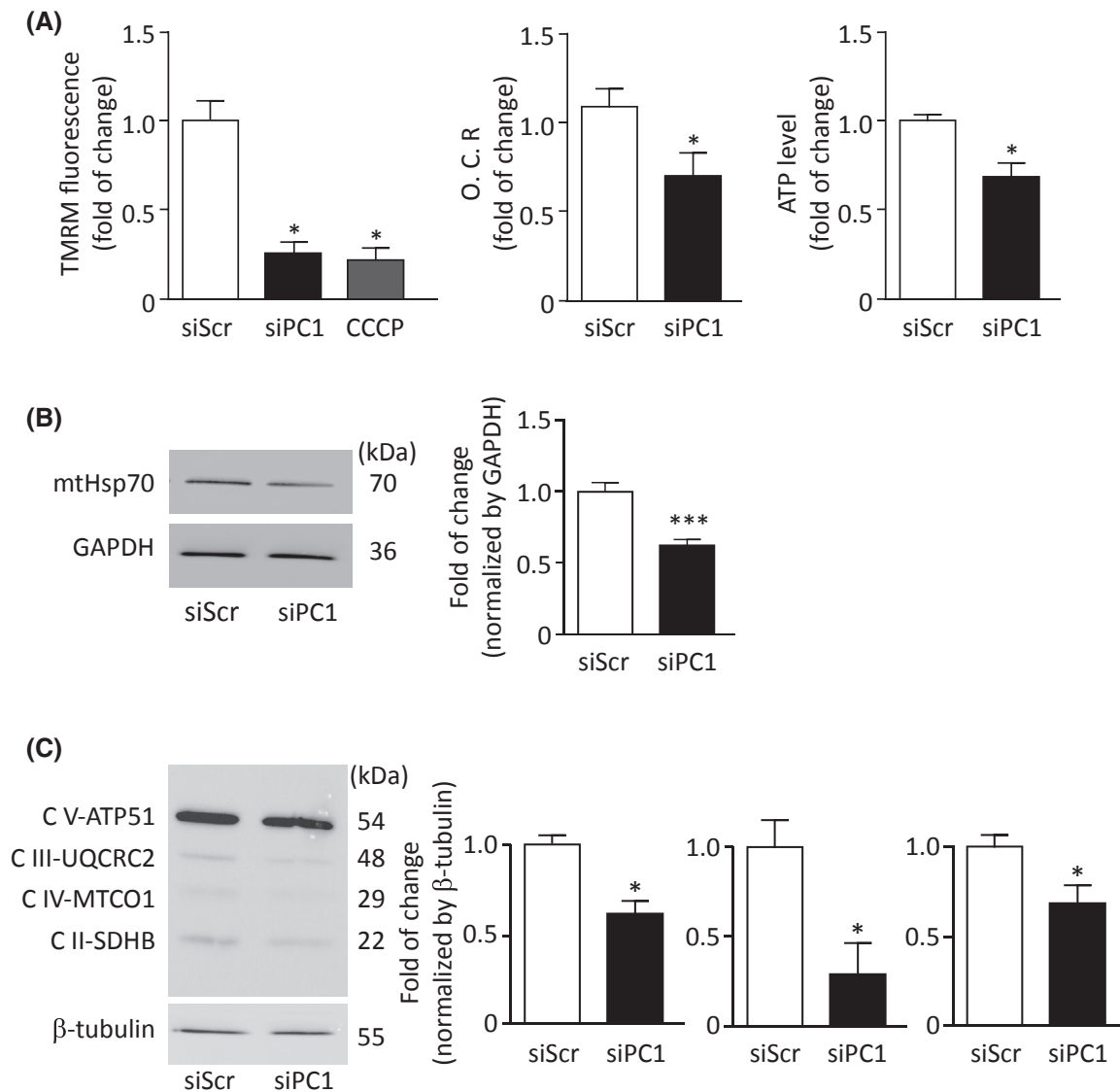


**FIGURE 1** Impaired oxidative metabolism in PC1 knockdown cardiomyocytes. A, PC1 knockdown and control (siScramble, siScr) NRVMs were incubated with tetramethylrhodamine (TMRM) to determine the mitochondrial membrane potential ( $\Psi_m$ ) through cytometry flow. CCCP (10  $\mu$ M) was used as a positive control of depolarization (left panel). The oxygen consumption rate (O. C. R.) of PC1 knockdown and control NRVM was evaluated with a Clark electrode (middle panel). Intracellular ATP content was determined using a luciferin-luciferase assay (right panel). B, Mitochondrial heat shock protein 70 (mtHsp70) levels were determined by Western blot in total protein extracts of cardiomyocytes. C, CII-SDHB, CIII-UQCRC2, and CIV-MTCO1 protein levels were determined by Western blot in total NRVM extracts. The left panel shows a representative Western blot image. Densitometry was quantified and relativized to  $\beta$ -tubulin levels. Images are representative of five independent experiments. Graphs represent mean  $\pm$  SEM. Statistical significance was calculated using the Student's unpaired *t* test, followed by the Tukey's test. \**P* < .05, \*\*\**P* < .001 vs siScr

potential ( $\Psi_m$ ) by 75% and basal oxygen consumption rate (O. C. R.) and total ATP levels, by 20%, with respect to controls (Figure 1A). In this set of experiments, CCCP, an uncoupling agent for mitochondrial respiration, was used as a positive control.

Given the evident alteration of parameters that characterize the functional state of mitochondria in NRVM knocked-down for PC1, we then evaluated whether these changes were related to a decrease of mitochondrial content.

As Figure 1B shows, the reduction of PC1 expression also reduced the expression of heat shock protein mtHsp70, a constitutive mitochondrial resident protein, and whose reduction is indicative of decreased total mitochondria mass. Likewise, we assessed whether OXPHOS expression was altered by PC1 knockdown, through the detection of NDUFB8-complex I, SDHB-complex II, UQCRC2-complex III, MTCO1-complex IV, and ATP5A-complex V subunits, which could explain the lower mitochondrial respiration

and ATP levels found. Our results indicate that the expression of subunits CV-ATP5 and CI-NDUFB8 remain unaltered (data not shown), while the expression of subunits CII-SDHB, CIII-UQCRC2, and CIV-MTCO1 was significantly decreased in NRVM (Figure 1C). To assess whether this lower expression of mitochondrial membrane proteins was related to a lower number of mitochondria produced by alterations of biogenesis, we evaluated if the reduction in PC1 protein levels modified the mitochondrial and nuclear DNA ratio and the levels of PGC-1 $\alpha$ , which is the master regulator of mitochondrial biogenesis. However, we found no significant differences compared to controls that could allow us to suspect that mitochondrial biogenesis was responsible for the changes produced by the absence of PC1 (Figure S2).

### 3.2 | Silencing of PC-1 expression eliminates damaged mitochondria

Mitophagy constitutes a key mitochondrial quality control mechanism that guarantees a rapid response to damage or physiological changes in the cell.<sup>23,24</sup> To evaluate whether PC1 knockdown activates mitophagy in NRVM, we measured changes in a panel of proteins that regulate this process. First, we observed that reduction of PC1 in NRVM increased protein levels of LC3B, an autophagosomal adapter protein used as a marker of autophagic activation (Figure 2A). We also evaluated the activation of specific organelle removal pathways mediated by the E3-ubiquitin ligase Parkin and PTEN-induced putative kinase 1 protein (PINK1). PINK1 is necessary for Parkin

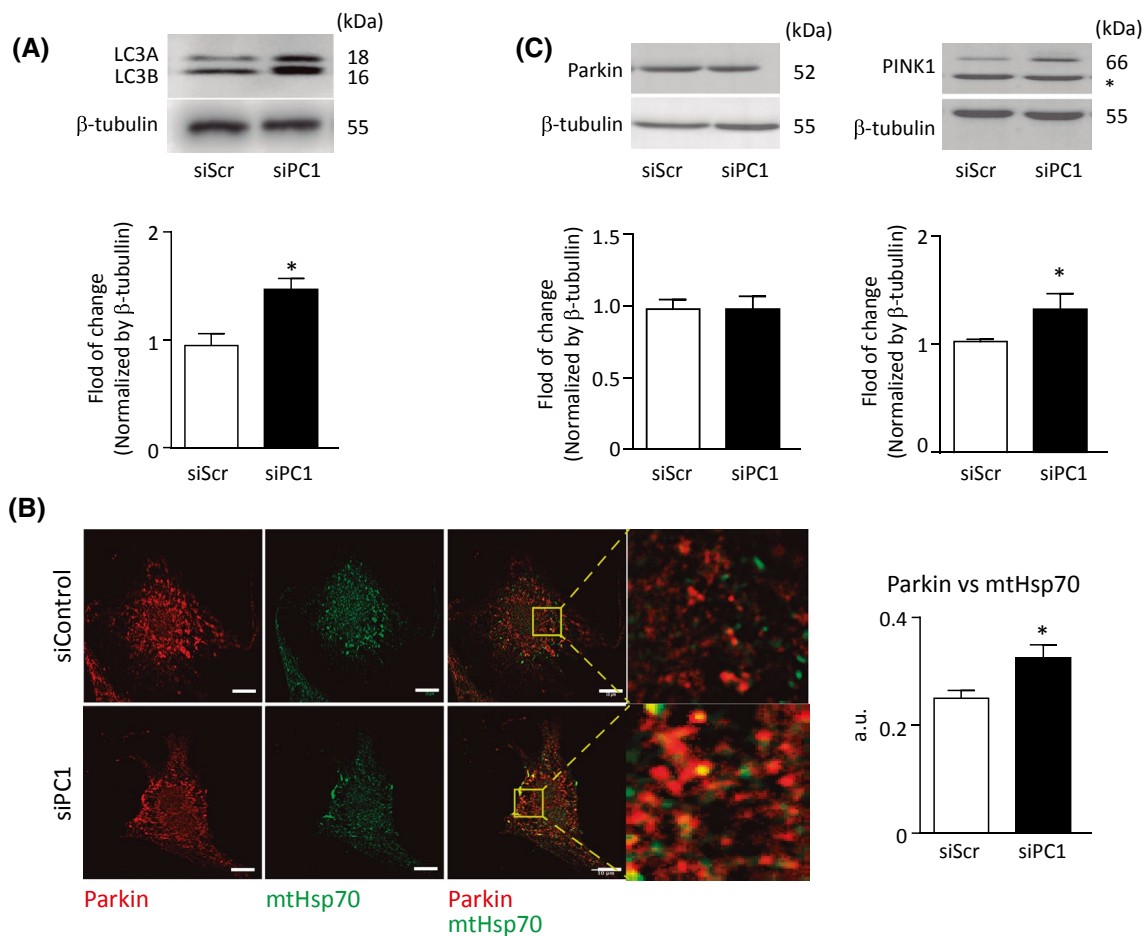


**FIGURE 2** Activation of mitophagy through the PINK1/Parkin pathway in PC1 knockdown cardiomyocytes. A, Levels of the autophagosomal adapter protein LC3B determined by Western blot in total cardiomyocyte extracts. Values were normalized to  $\beta$ -tubulin, relative to siScramble (siScr) control cells. B, Confocal images of immunodetection and fluorescence of Parkin (red) and mtHsp70 (green) in PC1 knockdown and siScr control cardiomyocytes (left panel). Scale bar: 20  $\mu$ m. Right images show magnification of colocalization. Parkin and mtHSP70 colocalization were calculated locally using Manders' coefficient (right panel). C, Parkin and PINK1 protein levels were determined by Western blotting in total NRVM extracts. Values were normalized to  $\beta$ -tubulin levels, relative to control siScr cells. All graphs represent mean  $\pm$  SEM of five independent experiments. Statistical significance was calculated using the Student's unpaired *t* test, followed by the Tukey's test. \**P* < .05 vs siScr

recruitment from the cytosol to the mitochondrial membrane to be phosphorylated and activated.<sup>26,36</sup> Parkin acts as an enhancer of mitophagy through further ubiquitination of mitochondrial proteins.<sup>37</sup> Through immunofluorescence assays, we evaluated the cellular distribution of Parkin (Figure 2B, left) and we also found a significant increment in the overlaying of Parkin over the mitochondrial network in PC1 knockdown cardiomyocytes, through an increment of Mander's coefficient (Figure 2B, right). Our results suggest that PINK1/Parkin-dependent mitophagy could be involved in the reduction of dysfunctional mitochondria elimination in PC1 knockdown cells. Thus, we also evaluated PINK1 and Parkin total protein levels, and we determined a significant increase of PINK1 but not Parkin (Figure 2C), which is consistent with activating this pathway and redistribution of Parkin to the mitochondrial membrane.

### 3.3 | PC1 silencing induces fission of the mitochondrial network

Mitophagy activation is related to alterations of mitochondrial network integrity and imbalance of mitochondrial dynamics. A more fissioned network has been related to an increase of mitophagy through different mechanisms.<sup>26</sup> To determine a possible alteration of mitochondrial dynamics that could explain the metabolic alterations produced by the reduction of PC1, we assessed mitochondrial morphology and expression of regulatory proteins, such as MFN2, OPA1, and Drp-1. Through confocal microscopy, we found that PC1 reduction led to a less connected mitochondrial network in NRVM (Figure 3A). Particle analysis showed that PC1 knockdown increased the number of mitochondria per cell but decreased the individual volume of mitochondria (Figure 3B), revealing that PC1 deficiency

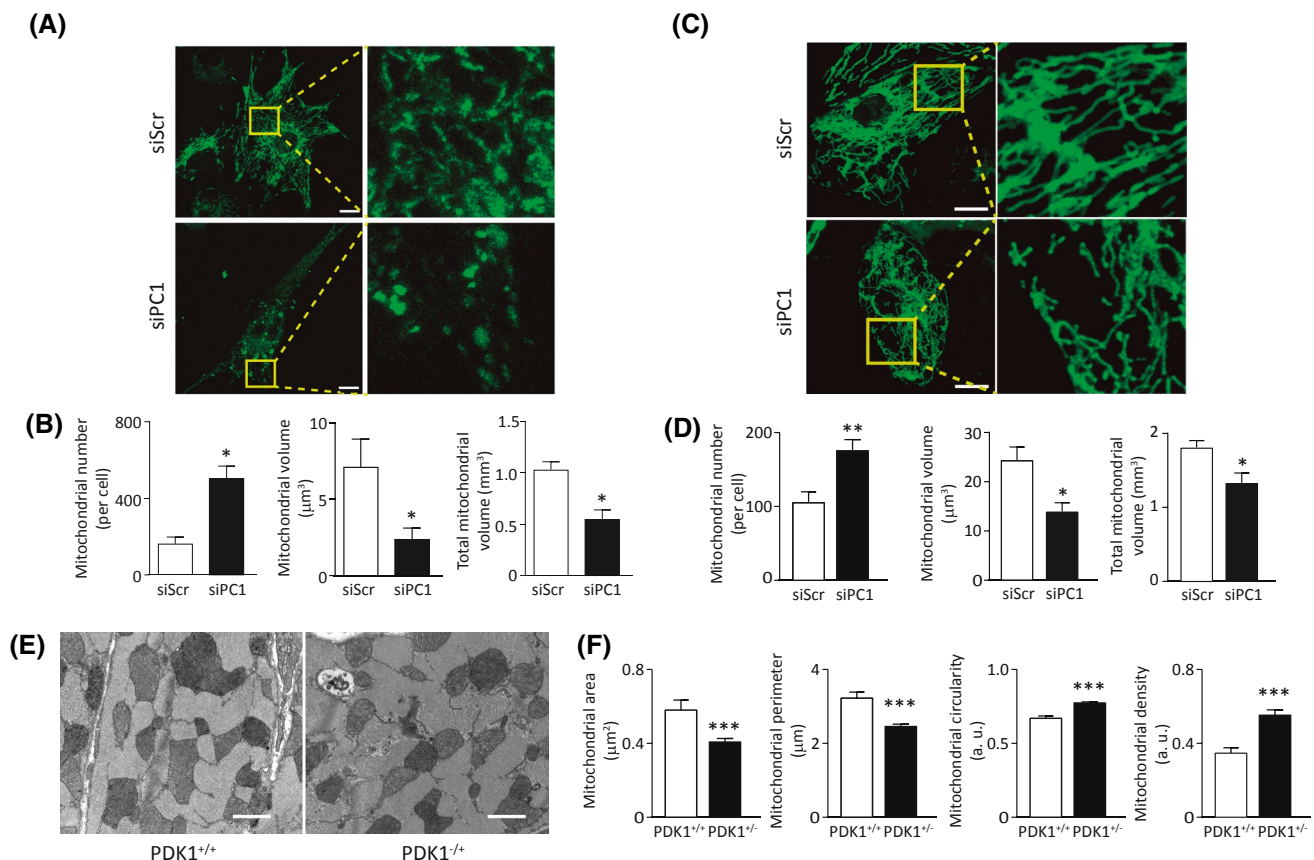
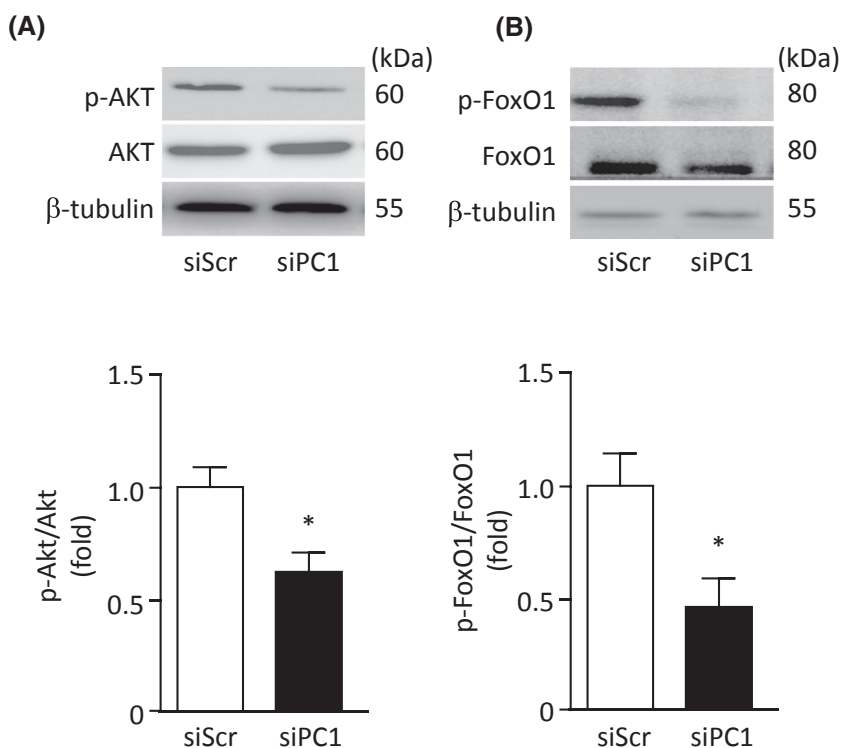


**FIGURE 3** Effects of PC1 silencing on mitochondrial morphology in cardiomyocytes. Confocal images of the mitochondrial network in (A) control and PC1 knockdown NRVM, and (B) control and PC1 knockdown human iPSC-derived cardiomyocytes stained with Mitotracker green (scale bar: 20  $\mu\text{m}$ ). The right panels show magnification and 3D reconstruction to determine the number and volume of mitochondrial particles. B and D, Quantitative analysis of the number of mitochondria per cell and mitochondrial volume was determined with the ImageJ software ( $n = 5$ ). E, Transmission electron microscopy images of homozygous Pkd1<sup>+/+</sup> (controls,  $n = 3$ ) and heterozygous Pkd1<sup>+/-</sup> ( $n = 3$ ) mice (scale bar: 1  $\mu\text{m}$ ). In total, 858 mitochondria were evaluated, with a minimum of 5 and a maximum of 27 mitochondria per image. Quantitative analysis of the mitochondrial area, perimeter, circularity, and density was determined with the ImageJ software. Graphs represent mean  $\pm$  SEM of independent experiments. Statistical significance was calculated using the Student's unpaired  $t$  test, followed by the Tukey's test. \* $P < .05$ , \*\* $P < .01$  vs siScr. \*\*\* $P < .001$  vs PDK1<sup>+/+</sup>



**FIGURE 4** Effects of PC1 silencing on AKT/FoxO1 pathway activation in cardiomyocytes. A, NRVMs were transduced with siPC1 and siScramble (siScr) and lysed 48 hours post-transduction to determine AKT activation through phospho Ser<sup>473</sup>-AKT/total AKT protein levels by Western blot. Quantification is presented below the images. B, FoxO1 activation was determined through phosphorylation on Ser<sup>256</sup>-FoxO1. Data are relative to total FoxO1 levels. Graphs represent mean  $\pm$  SEM of five independent experiments. Statistical significance was calculated using the Student's unpaired *t* test, followed by the Tukey's test. \**P* < .05 vs siScr



in cardiomyocytes promotes mitochondrial fission and reduction of total mitochondrial volume (Figure 3C), but without any significant change in Drp-1 phosphorylation or MFN2 and OPA1 protein levels (long and short forms) (Figure S3A-C). A similar result was also found in human iPSC-derived cardiomyocytes. PC1 knockdown triggers an increase in the mitochondrial number per cell with a decrease in their volume (Figure 3C,D). Interestingly, both cellular models, NRVMs and iPSC-derived cardiomyocytes, also reduced the total mitochondrial volume (Figure 3B,D), which is consistent with the mitophagy results obtained in Figure 2. Moreover, heterozygous cardiomyocyte-specific PDK-1<sup>+/-</sup> mice with a 50% reduction in PC1 protein level also displayed smaller mitochondria, with reduced area and perimeter, and increased mitochondrial circularity and density, as visualized by transmission electron microscopy of heart samples (Figure 3E). These results suggest that a 50% reduction of PC-1 level is sufficient to induce mitochondrial fission.

### 3.4 | The absence of PC1 deregulates phosphorylation of the AKT-FoxO1 pathway

Previous studies in cardiomyocytes have shown that the phosphorylation of AKT in Ser<sup>473</sup> depends on PC1 expression,<sup>20</sup> and its downstream effector FoxO1,<sup>38</sup> which also regulates PINK1/Parkin-dependent mitophagy.<sup>39,40</sup>

Based on these antecedents, we evaluated if PC1 reduction affected phosphorylation of AKT (Ser<sup>473</sup>) and FoxO1 (Ser<sup>256</sup>).<sup>41</sup> Our results show that PC1 reduction did not change AKT and FoxO1 total protein levels but significantly decreased the phosphorylation of AKT (Figure 4A) and FoxO1 (Figure 4B). Previous studies suggest that PC1 regulates the stabilization of L-type calcium channels.<sup>20</sup> However, the decrease of AKT and FoxO1 phosphorylation was not due to the L-type calcium channel because of its inhibition with nifedipine, which triggers mitochondrial fission (Figure S4A-C), did not increase AKT (Ser<sup>473</sup>) and FoxO1 (Ser<sup>256</sup>) phosphorylation (Figure S4D,E).

### 3.5 | FoxO1 also alters metabolism and induces fragmentation of the mitochondrial network

To validate whether the mitochondrial metabolism and morphological dysregulations seen in PC1 knockdown cells were triggered by the dysregulation of the AKT-FoxO1 axis, we evaluated if these alterations were replicated by sustained activation of FoxO1. To this end, we performed the transduction and overexpression of a constitutively active form of FoxO1 (FoxO1-CA), as previously described.<sup>41</sup> NRVM transduced with MOI 10 and MOI 25 showed an increase in the levels of FoxO1-GFP constructs (control and constitutively active), with the absence of FoxO1-CA phosphorylation (Figure S5A),

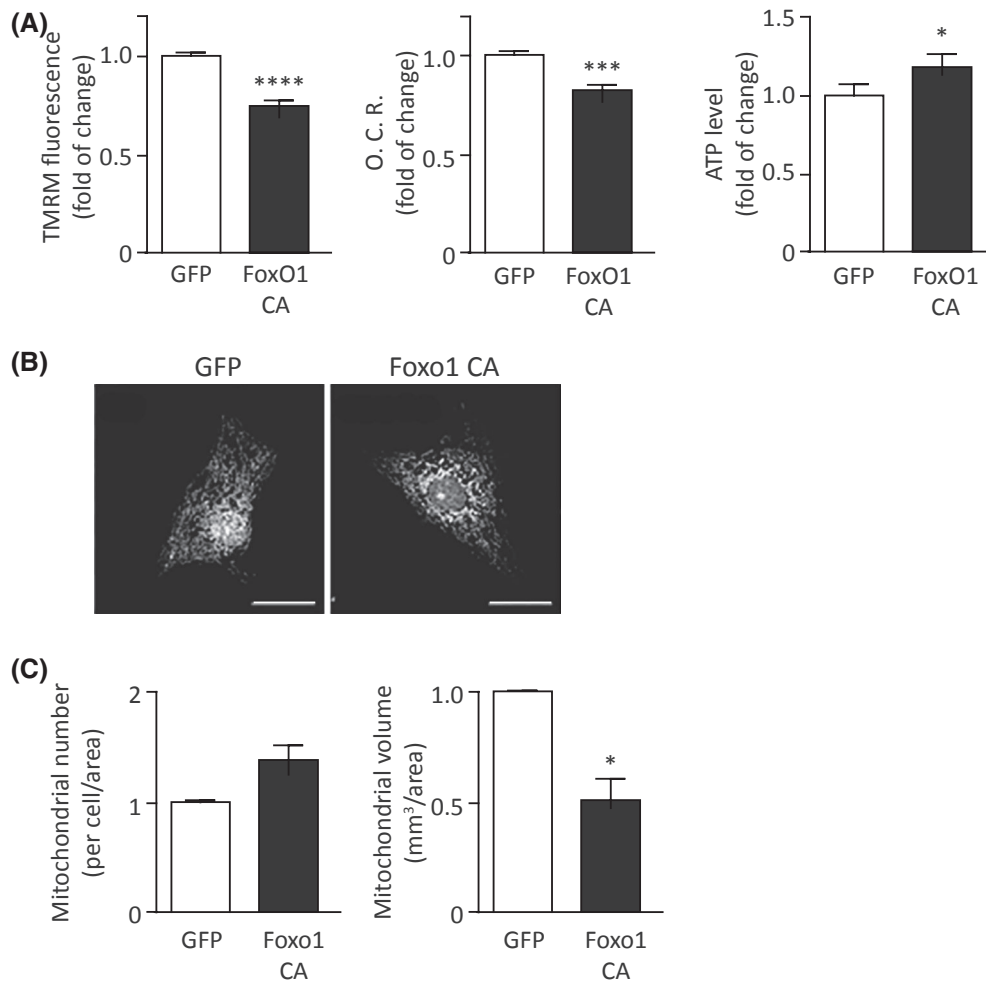


**FIGURE 5** Effects of sustained activation of FoxO1 on metabolic parameters and mitochondrial network morphology in cardiomyocytes. A, NRVMs were transduced with adenovirus that overexpressed GFP or FoxO1 constitutively active-GFP (FoxO1 CA). Forty-eight hours post-transduction, the cells were incubated with tetramethylrhodamine (TMRM) for 30 minutes to determine the mitochondrial membrane potential ( $\Psi_m$ ) through flow cytometry ( $n = 7$ , left panel). The oxygen consumption rate (O. C. R.) of NRVM that overexpressed GFP or FoxO1 CA was evaluated with a Clark electrode ( $n = 5$ , middle panel). Intracellular ATP content of GFP or FoxO1 CA cardiomyocytes was determined using the Cell Titer-Glo kit ( $n = 8$ , right panel). B, Representative confocal images of the mitochondrial network in NRVM that overexpressed GFP or FoxO1 CA by 48 hours. Cells were stained with MitoTracker Orange for 30 minutes. Confocal images were subjected to 3D reconstruction. ( $n = 4$ , Scale bar: 10  $\mu$ m). C, Quantitative analysis of mitochondrial morphology in NRVM that expressed GFP or FoxO1 CA by 48 hours. Number of mitochondria per cell and mitochondrial volume were evaluated with the ImageJ software and normalized by cell area ( $n = 4$ ). Graphs represent mean  $\pm$  SEM of four independent experiments. Statistical significance was calculated using the Student's unpaired  $t$  test, followed by the Tukey's test. \* $P < .05$ , \*\*\* $P < .001$  \*\*\*\* $P < .0001$ , vs GFP

with a predominantly nuclear distribution (Figure S5B) and a significant increase in the expression of *Atrogin*, a recognized target gene of FoxO1 (Figure S5C). As in PC1 knockdown cells, the overexpression of FoxO1-CA decreased mitochondrial membrane potential and oxygen consumption rate; however, ATP levels in this model were increased (Figure 5A), but mitochondrial morphology was affected as well (Figure 5B). We also observed that those cells that overexpressed FoxO1-CA showed a trend toward an increase in the number of mitochondria per cell but with a significant lower volume (Figure 5B,C).

### 3.6 | The absence of PC1 activates mitophagy in cardiomyocytes in a FoxO1-dependent manner

To verify if mitophagy activation occurred in response to decreased FoxO1 phosphorylation in PC1 knockdown cells, we performed a double knockdown against PC1 and FoxO1 in NRVM (Figure S6) and evaluated changes in subcellular Parkin location and mitochondrial morphological changes. By confocal microscopy and the determination of Mander's coefficient, we quantified the degree of Parkin and mtHSP70 colocalization and found

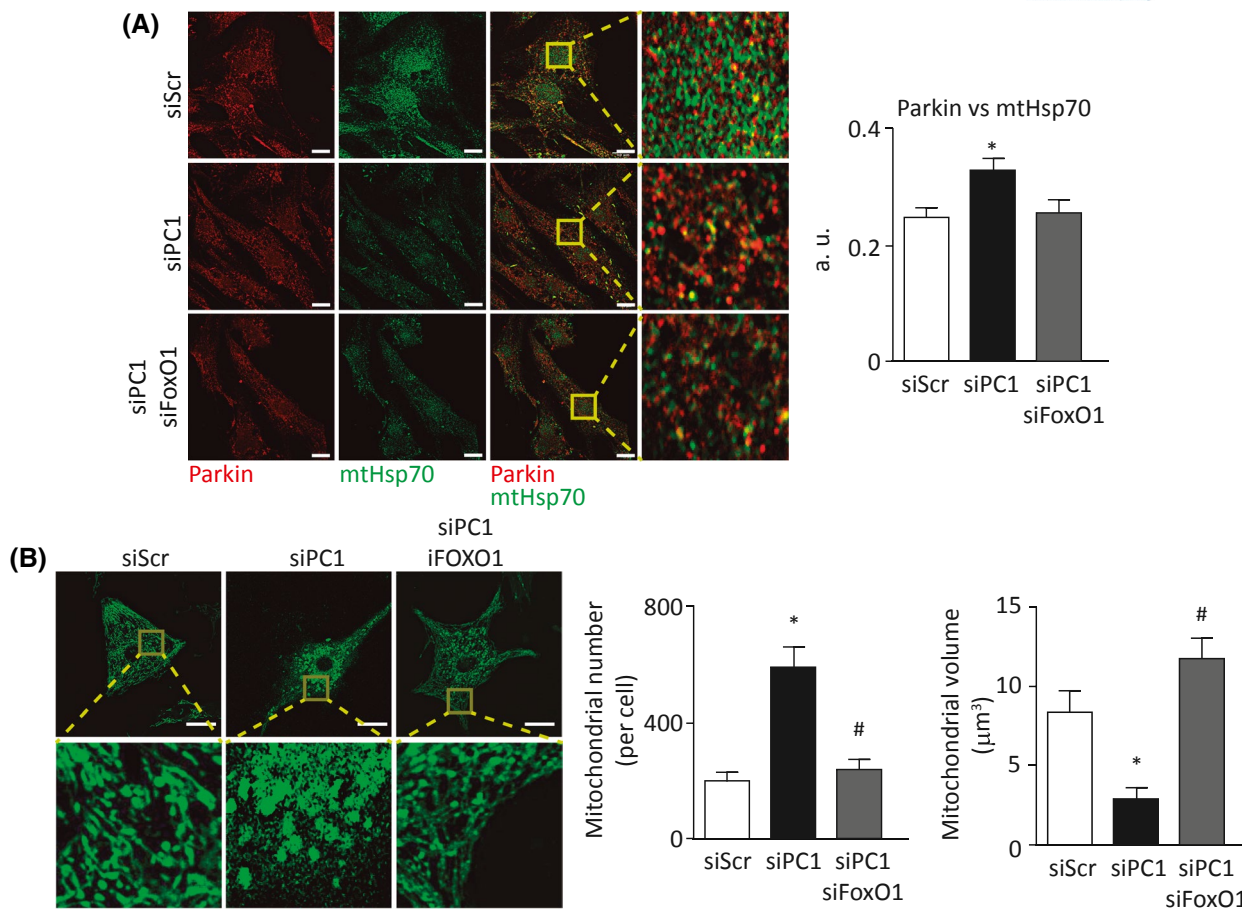


**FIGURE 6** Rescue of mitophagy and recovery of mitochondrial morphology through FoxO1 silencing in PC1 knockdown cardiomyocytes. A, Representative confocal images of immunodetection and fluorescence of Parkin (red), mtHsp70 (green), and merge in PC1-FoxO1 double knockdown and control (siScramble, siScr) NRVM (scale bar: 20  $\mu\text{m}$ , left panel). Right images show magnification of colocalization. Parkin and mtHSP70 colocalization were calculated locally using Manders' coefficient (right panel). B, Representative confocal images of the mitochondrial network in PC1-FoxO1 double knockdown and control NRVM, stained with Mitotracker green (scale bar: 20  $\mu\text{m}$ , left panel). The images at the bottom show magnification of selected square sections. Quantitative analysis of the number of mitochondria per cell and mitochondrial volume, determined with the ImageJ software. Graphs represent mean  $\pm$  SEM of five independent experiments. Statistical significance was calculated using one-way ANOVA, followed by the Tukey's test. \* $P < .05$  vs siScr, # $P < .05$  vs siPC1. \* $P < .05$  vs siScr

that the reduction of FoxO1 expression avoided Parkin recruitment (Figure 6A) and mitochondrial network fragmentation (Figure 6B) induced by PC1 knockdown. Reduction of FoxO1 not only significantly decreased the mitochondrial number per cell but also the average volume of mitochondria (Figure 6B). These results suggest that the ablation of PC1 in NRVM leads to clearance of dysfunctional mitochondria, a process that could be related to the reduction of AKT phosphorylation, followed by a decrease of FoxO1 phosphorylation and subsequent activation of PINK1/Parkin-dependent mitophagy.

#### 4 | DISCUSSION

The enormous energy requirements of cardiomyocytes make them highly sensitive to changes in intracellular

metabolism. Mitochondria are crucial for ATP production, and the dynamic processes of fusion, fission, biogenesis, and degradation regulate their availability and morphology and, therefore, their function.

Studies suggest that PC1 has a pivotal role in the contractility of the heart, by directly modulating the stabilization of L-type calcium channels and action potentials in cardiomyocytes<sup>3,7</sup>; however, until now, its role in the regulation of mitochondrial metabolism and dynamics was unknown. In this study, we established that PC1 in NRVM modulates the dynamics and functionality of mitochondria by showing that alterations in the expression of this protein generate a dysregulation of the AKT/FoxO1 pathway, thus over-activating mitophagy.

The AKT-FoxO1 pathway is related to vital cellular processes, such as proliferation, cell cycle, and apoptosis, among others,<sup>3,20</sup> and in cardiac tissue, the active form of

AKT (phospho-AKT) promotes mitochondrial fusion.<sup>42</sup> In the same line, our results established that PC1 down-regulation reduces the phosphorylation of AKT in Ser<sup>473</sup> and of FoxO1 in Ser<sup>256</sup>, which could explain the increase in mitochondrial fission and mitophagy activation. This could be due, in part, to the relation between AKT activation and the phosphorylation of pro-survival Bcl-2 family members, which induce the efflux of mitochondrial content and activation of the PINK1/Parkin mitophagy pathway.<sup>43-45</sup>

In a complementary line, overexpression of a constitutively active form of FoxO1 (FoxO1-CA)—which is predominantly nuclear because it is not under AKT inhibitory control<sup>41</sup>—showed similar results to those obtained in PC1 knockdown cardiomyocytes, with a reduction in mitochondrial membrane potential and oxygen consumption rate and an increase in mitochondrial fission. However, sustained FoxO1 activation also generates a dysregulation of AKT phosphorylation, suppression of protein phosphatase 2A (PP2A), and disruption of AKT-PP2A and AKT-calcineurin interactions, as well as reduction of insulin sensitivity, and consequent glucose metabolism impairment<sup>41</sup>; these factors could explain the discordance between ATP levels in the PC1 knockdown with respect to the FoxO1-CA cells. FoxO1 also regulates genes involved in cellular homeostasis, cellular quality control, and metabolism.<sup>38,46-48</sup> Furthermore, FoxO1 activation induces mitophagy by activating E3-ubiquitin ligase Mub1 and the PINK1/Parkin pathway.<sup>49</sup> Our results suggest that mitophagy produced in PC1 knockdown cardiomyocytes could be modulated by FoxO1 through the PINK1/Parkin pathway. FoxO1 silencing reverses the recruitment of Parkin to the mitochondria and recovers, in part, mitochondrial network morphology. The rescue and recovery of mitochondrial morphology are essential, considering that mitophagy imbalance has been related to the development of diverse cardiac pathologies.<sup>50-52</sup> By establishing a timeline, we could consider the increase in the expression levels of PINK1 in PC1 knockdown cardiomyocytes as a pro-fission and regulatory signal of mitophagy, as previously described,<sup>53</sup> resulting in a decrease of mitochondrial mass due to the loss of connectivity of the mitochondrial network. This would allow the assembly of the mitophagy machinery, such as the recruitment of Parkin to the mitochondrial membrane and an increase in the expression levels of adapter proteins of the autophagosome, and finally, the selective elimination of mitochondria. A time longer than 48 hours in the mtDNA evaluation would allow us to complement the data obtained in this study, which by not showing significant changes could indicate that 48 hours are not enough to carry out the elimination of such a large number of mitochondria as to be reflected in a substantial decrease in mtDNA. It would be

interesting in future research to consider more long-term effects that also address parameters related to dysregulation of mitophagy and cell death, which are also broadly linked to the development of cardiac pathologies.<sup>54</sup>

Although until now there are no studies that directly relate *Pdk1* mutations with mitochondrial metabolism in cardiac tissue, ADPKD patients, and animal models of polycystic kidney disease exhibit a tissue-dependent metabolic dysregulation,<sup>1,35,55</sup> establishing a direct relationship between changes in PC1 expression and mitochondrial metabolic and morphological changes. In these studies, patients with obesity and diabetes show faster progress in terms of cyst formation and renal dysfunction, in addition to inadequate management of glucose and oxidative metabolism.<sup>31</sup> Other studies in cell models, such as epithelial and kidney cell lines, have indicated that the C-terminal domain of PC1 is cleaved and migrates to the mitochondrial matrix to modulate fatty acid oxidation.<sup>9</sup> Additionally, altered expression of PC1 generates a loss of the connectivity of the mitochondrial network and dysfunction in the marker parameters of oxidative metabolism.<sup>10,11</sup> Our results agree with these observations, and we also found dysregulation of the AKT-FoxO1 axis, a pathway of great importance for the response to insulin and management of glucose levels.<sup>13,19</sup>

The mechanism through which PC1 regulates metabolism is not completely clear now; however, our work contributes to the knowledge of PC1 functions in the heart, showing that it is not only involved in contractile function but also in the regulation of metabolic processes dependent on mitochondria. This work provides valuable information about extra-renal symptoms reported for patients with ADPKD and their novel therapeutic intervention.

## ACKNOWLEDGMENTS

The authors thank Gindra Latorre and Fidel Albornoz for their excellent technical support. This work was supported by the Agencia Nacional de Investigación y Desarrollo (ANID), Chile, Grant/Award Numbers: FONDECYT 3190546, 1190743, 1200490, 1180613, 3210443, 3210496, FONDAPE 15130011, and PhD fellowships 21191341 and 21171588; International Centre for Genetic Engineering and Biotechnology (ICGEB), Grant/Award Number: CRP/CHL18-04; University of Chile grant U-Redes Generación, Grant/Award Number: VID G\_2018-35, Houston Methodist Start-Up funds.

## DISCLOSURES

All authors declare no conflicts of interest.

## AUTHOR CONTRIBUTIONS

A. Ramírez-Sagredo, C. Quiroga, F. Altamirano, V. Parra, Z. Pedrozo, M. Chiong, and S. Lavandero



designed the research; C. Quiroga, V. Parra, F. Altamirano, Z. Pedrozo, M. Chiong, and S. Lavandero supervised the project; and A. Ramírez-Sagredo, V. Garrido-Moreno, C. López-Crisosto, S. Leiva-Navarrete, I. Norambuena-Soto, M.C. Díaz-Vesga, W.A. Perez, T. Hendrickson, and J. Ortiz-Quintero performed the research. Data were analyzed and thoroughly discussed by A. Ramírez-Sagredo, C. Quiroga, F. Altamirano, V. Parra, Z. Pedrozo, M. Chiong, and S. Lavandero. The manuscript was written by A. Ramírez-Sagredo, C. Quiroga, V. Parra, F. Altamirano, Z. Pedrozo, M. Chiong, and S. Lavandero and approved by all the authors.

## ORCID

Andrea Ramírez-Sagredo  <https://orcid.org/0000-0003-1081-0704>

Clara Quiroga  <https://orcid.org/0000-0002-0251-4772>

Valeria Garrido-Moreno  <https://orcid.org/0000-0002-3298-2622>

Camila López-Crisosto  <https://orcid.org/0000-0003-1055-099X>

Ignacio Norambuena-Soto  <https://orcid.org/0000-0002-2676-2674>


Magda C. Díaz-Vesga  <https://orcid.org/0000-0002-7807-2050>

William Perez  <https://orcid.org/0000-0003-0344-4160>

Troy Hendrickson  <https://orcid.org/0000-0001-6773-4410>

Valentina Parra <http://orcid.org/0000-0002-0080-6472>

Zully Pedrozo  <https://orcid.org/0000-0003-4690-2803>

Francisco Altamirano  <https://orcid.org/0000-0002-1612-2729>

Mario Chiong  <https://orcid.org/0000-0002-5174-6545>

Sergio Lavandero  <https://orcid.org/0000-0003-4258-1483>

## REFERENCES

- Menezes LF, Germino GG. The pathobiology of polycystic kidney disease from a metabolic viewpoint. *Nat Rev Nephrol.* 2019;15:735-749.
- Torres VE, Harris PC, Pirson Y. Autosomal dominant polycystic kidney disease. *Lancet.* 2007;369:1287-1301.
- Altamirano F, Schiattarella GG, French KM, et al. Polycystin-1 assembles with Kv channels to govern cardiomyocyte repolarization and contractility. *Circulation.* 2019;140:921-936.
- Klawitter J, Reed-Gitomer BY, McFann K, et al. Endothelial dysfunction and oxidative stress in polycystic kidney disease. *Am J Physiol Renal Physiol.* 2014;307:F1198-F1206.
- Menon V, Rudym D, Chandra P, Miskulin D, Perrone R, Sarnak M. Inflammation, oxidative stress, and insulin resistance in polycystic kidney disease. *Clin J Am Soc Nephrol.* 2011;6:7-13.
- Chebib FT, Hogan MC, El-Zoghby ZM, et al. Autosomal dominant polycystic kidney patients may be predisposed to various cardiomyopathies. *Kidney Int Rep.* 2017;2:913-923.
- Pedrozo Z, Criollo A, Battiprolu PK, et al. Polycystin-1 is a cardiomyocyte mechanosensor that governs L-type Ca<sup>2+</sup> channel protein stability. *Circulation.* 2015;131:2131-2142.
- Padovano V, Kuo IY, Stavola LK, et al. The polycystins are modulated by cellular oxygen-sensing pathways and regulate mitochondrial function. *Mol Biol Cell.* 2017;28:261-269.
- Lin CC, Kurashige M, Liu Y, et al. A cleavage product of Polycystin-1 is a mitochondrial matrix protein that affects mitochondria morphology and function when heterologously expressed. *Sci Rep.* 2018;8:2743.
- Ishimoto Y, Inagi R, Yoshihara D, et al. Mitochondrial abnormality facilitates cyst formation in autosomal dominant polycystic kidney disease. *Mol Cell Biol.* 2017;37:e00337-e00317.
- Menezes LF, Lin CC, Zhou F, Germino GG. Fatty acid oxidation is impaired in an orthologous mouse model of autosomal dominant polycystic kidney disease. *EBioMedicine.* 2016;5:183-192.
- Zhan M, Brooks C, Liu F, Sun L, Dong Z. Mitochondrial dynamics: regulatory mechanisms and emerging role in renal pathophysiology. *Kidney Int.* 2013;83:568-581.
- Barthel A, Schmoll D, Unterman TG. FoxO proteins in insulin action and metabolism. *Trends Endocrinol Metab.* 2005;16:183-189.
- Zhang W, Patil S, Chauhan B, et al. FoxO1 regulates multiple metabolic pathways in the liver: effects on gluconeogenic, glycolytic, and lipogenic gene expression. *J Biol Chem.* 2006;281:10105-10117.
- Ning Y, Li Z, Qiu Z. FOXO1 silence aggravates oxidative stress-promoted apoptosis in cardiomyocytes by reducing autophagy. *J Toxicol Sci.* 2015;40:637-645.
- Wang D, Wang Y, Zou X, et al. FOXO1 inhibition prevents renal ischemia-reperfusion injury via cAMP-response element binding protein/PPAR-gamma coactivator-1alpha-mediated mitochondrial biogenesis. *Br J Pharmacol.* 2020;177:432-448.
- Shi Y, Fan S, Wang D, et al. FOXO1 inhibition potentiates endothelial angiogenic functions in diabetes via suppression of ROCK1/Drp1-mediated mitochondrial fission. *Biochim Biophys Acta Mol Basis Dis.* 2018;1864:2481-2494.
- Sanchez AM, Candau RB, Bernardi H. FoxO transcription factors: their roles in the maintenance of skeletal muscle homeostasis. *Cell Mol Life Sci.* 2014;71:1657-1671.
- Matsuzaki H, Daitoku H, Hatta M, Tanaka K, Fukamizu A. Insulin-induced phosphorylation of FKHR (Foxo1) targets to proteasomal degradation. *Proc Natl Acad Sci U S A.* 2003;100:11285-11290.
- Cordova-Casanova A, Olmedo I, Riquelme JA, et al. Mechanical stretch increases L-type calcium channel stability in cardiomyocytes through a polycystin-1/AKT-dependent mechanism. *Biochim Biophys Acta Mol Cell Res.* 2018;1865:289-296.
- Pennanen C, Parra V, Lopez-Crisosto C, et al. Mitochondrial fission is required for cardiomyocyte hypertrophy mediated by a Ca<sup>2+</sup>-calcineurin signaling pathway. *J Cell Sci.* 2014;127:2659-2671.
- Jasova M, Kancirova I, Waczulikova I, Ferko M. Mitochondria as a target of cardioprotection in models of preconditioning. *J Bioenerg Biomembr.* 2017;49:357-368.
- Kubli DA, Cortez MQ, Moyzis AG, Najor RH, Lee Y, Gustafsson AB. PINK1 is dispensable for mitochondrial recruitment of parkin and activation of mitophagy in cardiac myocytes. *PLoS ONE.* 2015;10:e0130707.

24. Trotta AP, Chipuk JE. Mitochondrial dynamics as regulators of cancer biology. *Cell Mol Life Sci.* 2017;74:1999-2017.
25. Di Lisa F, Bernardi P. Mitochondria and ischemia-reperfusion injury of the heart: fixing a hole. *Cardiovasc Res.* 2006;70:191-199.
26. Yoo SM, Jung YK. A molecular approach to mitophagy and mitochondrial dynamics. *Mol Cells.* 2018;41:18-26.
27. Galvez A, Morales MP, Eltit JM, et al. A rapid and strong apoptotic process is triggered by hyperosmotic stress in cultured rat cardiac myocytes. *Cell Tissue Res.* 2001;304:279-285.
28. Boudina S, Sena S, Theobald H, et al. Mitochondrial energetics in the heart in obesity-related diabetes: direct evidence for increased uncoupled respiration and activation of uncoupling proteins. *Diabetes.* 2007;56:2457-2466.
29. Munoz JP, Chiong M, Garcia L, et al. Iron induces protection and necrosis in cultured cardiomyocytes: role of reactive oxygen species and nitric oxide. *Free Radic Biol Med.* 2010;48:526-534.
30. Chiong M, Parra V, Eisner V, et al. Parallel activation of Ca(2+)-induced survival and death pathways in cardiomyocytes by sorbitol-induced hyperosmotic stress. *Apoptosis.* 2010;15:887-903.
31. Yoon Y, Krueger EW, Oswald BJ, McNiven MA. The mitochondrial protein hFis1 regulates mitochondrial fission in mammalian cells through an interaction with the dynamin-like protein DLP1. *Mol Cell Biol.* 2003;23:5409-5420.
32. Hong T, Yang H, Zhang SS, et al. Cardiac BIN1 folds T-tubule membrane, controlling ion flux and limiting arrhythmia. *Nat Med.* 2014;20:624-632.
33. Parra V, Altamirano F, Hernandez-Fuentes CP, et al. Down syndrome critical region 1 gene, Rcan1, helps maintain a more fused mitochondrial network. *Circ Res.* 2018;122:e20-e33.
34. Parra V, Verdejo HE, Iglewski M, et al. Insulin stimulates mitochondrial fusion and function in cardiomyocytes via the Akt-mTOR-NFkappaB-OPA-1 signaling pathway. *Diabetes.* 2014;63:75-88.
35. Rowe I, Chiaravalli M, Mannella V, et al. Defective glucose metabolism in polycystic kidney disease identifies a new therapeutic strategy. *Nat Med.* 2013;19:488-493.
36. Nguyen TN, Padman BS, Lazarou M. Deciphering the molecular signals of pink1/parkin mitophagy. *Trends Cell Biol.* 2016;26:733-744.
37. Pernas L, Scorrano L. Mito-morphosis: mitochondrial fusion, fission, and cristae remodeling as key mediators of cellular function. *Annu Rev Physiol.* 2016;78:505-531.
38. Brunet A, Bonni A, Zigmond MJ, et al. AKT promotes cell survival by phosphorylating and inhibiting a Forkhead transcription factor. *Cell.* 1999;96:857-868.
39. Li W, Du M, Wang Q, et al. FoxO1 Promotes mitophagy in the podocytes of diabetic male mice via the pink1/parkin pathway. *Endocrinology.* 2017;158:2155-2167.
40. Sengupta A, Molkenin JD, Yutzey KE. FoxO transcription factors promote autophagy in cardiomyocytes. *J Biol Chem.* 2009;284:28319-28331.
41. Ni YG, Wang N, Cao DJ, et al. FoxO transcription factors activate AKT and attenuate insulin signaling in heart by inhibiting protein phosphatases. *Proc Natl Acad Sci U S A.* 2007;104:20517-20522.
42. Stiles BL. PI-3-K and AKT: onto the mitochondria. *Adv Drug Deliv Rev.* 2009;61:1276-1282.
43. Nechushtan A, Smith CL, Hsu YT, Youle RJ. Conformation of the Bax C-terminus regulates subcellular location and cell death. *EMBO J.* 1999;18:2330-2341.
44. Datta SR, Dudek H, Tao X, et al. AKT phosphorylation of BAD couples survival signals to the cell-intrinsic death machinery. *Cell.* 1997;91:231-241.
45. Bravo-San Pedro JM, Kroemer G, Galluzzi L. Autophagy and mitophagy in cardiovascular disease. *Circ Res.* 2017;120:1812-1824.
46. Vivanco I, Sawyers CL. The phosphatidylinositol 3-kinase AKT pathway in human cancer. *Nat Rev Cancer.* 2002;2:489-501.
47. Wallace DP. Cyclic AMP-mediated cyst expansion. *Biochim Biophys Acta.* 2011;1812:1291-1300.
48. Rabinowitz JD, White E. Autophagy and metabolism. *Science.* 2010;330:1344-1348.
49. Puri R, Cheng XT, Lin MY, Huang N, Sheng ZH. Mulf1 restrains Parkin-mediated mitophagy in mature neurons by maintaining ER-mitochondrial contacts. *Nat Commun.* 2019;10:3645.
50. Huang CY, Lai CH, Kuo CH, et al. Inhibition of ERK-Drp1 signaling and mitochondria fragmentation alleviates IGF-IIR-induced mitochondria dysfunction during heart failure. *J Mol Cell Cardiol.* 2018;122:58-68.
51. Marin-Garcia J, Akhmedov AT. Mitochondrial dynamics and cell death in heart failure. *Heart Fail Rev.* 2016;21:123-136.
52. Yang M, Linn BS, Zhang Y, Ren J. Mitophagy and mitochondrial integrity in cardiac ischemia-reperfusion injury. *Biochim Biophys Acta Mol Basis Dis.* 2019;1865:2293-2302.
53. Pryde KR, Smith HL, Chau KY, Schapira AH. PINK1 disables the anti-fission machinery to segregate damaged mitochondria for mitophagy. *J Cell Biol.* 2016;213:163-171.
54. Morales PE, Arias-Duran C, Avalos-Guajardo Y, et al. Emerging role of mitophagy in cardiovascular physiology and pathology. *Mol Aspects Med.* 2020;71:100822.
55. Mangoo-Karim R, Uchic ME, Grant M, et al. Renal epithelial fluid secretion and cyst growth: the role of cyclic AMP. *FASEB J.* 1989;3:2629-2632.

## SUPPORTING INFORMATION

Additional Supporting Information may be found online in the Supporting Information section.

**How to cite this article:** Ramirez-Sagredo A, Quiroga C, Garrido-Moreno V, et al. Polycystin-1 regulates cardiomyocyte mitophagy. *FASEB J.* 2021;35:e21796. <https://doi.org/10.1096/fj.202002598R>